THE JOURNAL OF BIOLOGICAL CHEMISTRY
Vol. 280, No. 32, Issue of August 12, pp. 29169–29175, 2005
Printed in U.S.A.

The Apical Targeting Signal of the $P2Y_2$ Receptor Is Located in Its First Extracellular Loop*

Received for publication, February 3, 2005, and in revised form, May 19, 2005
Published, JBC Papers in Press, May 20, 2005, DOI 10.1074/jbc.M501301200

Ai-Dong Qi, Samuel C. Wolff, and Robert A. Nicholas‡

From the Department of Pharmacology, The University of North Carolina at Chapel Hill, Chapel Hill, North Carolina 27599-7365

$P2Y_2$ and $P2Y_4$ receptors, which have 52% sequence identity, are both expressed at the apical membrane of Madin-Darby canine kidney cells, but the locations of their apical targeting signals are distinctly different. The targeting signal of the $P2Y_2$ receptor is located between the N terminus and 7TM, whereas that of the $P2Y_4$ receptor is present in its C-terminal tail. To identify the apical targeting signal in the $P2Y_2$ receptor, regions of the $P2Y_2$ receptor were progressively substituted with the corresponding regions of the $P2Y_4$ receptor lacking its targeting signal. Characterization of these chimeras and subsequent mutational analysis revealed that four amino acids (Arg^{95}, Gly^{96}, Asp^{97}, and Leu^{108}) in the first extracellular loop play a major role in apical targeting of the $P2Y_2$ receptor. Mutation of RGD to RGE had no effect on $P2Y_2$ receptor targeting, indicating that receptor-integrin interactions are not involved in apical targeting. $P2Y_2$ receptor mutants were localized in a similar manner in Caco-2 colon epithelial cells. This is the first identification of an extracellular protein-based targeting signal in a seven-transmembrane receptor.

Extracellular nucleotides play an important role in a broad range of physiological and pathophysiological processes through two classes of receptors, the ligand-gated P2X receptors and the G protein-coupled P2Y receptors (1, 2). To date, pharmacological characterization and molecular cloning have identified seven P2X receptors ($P2X_{1–7}$) and eight P2Y receptor subtypes ($P2Y_1$, $P2Y_2$, $P2Y_4$, $P2Y_6$, $P2Y_{11}$, $P2Y_{12}$, $P2Y_{13}$, and $P2Y_{14}$). The P2Y receptors can be divided into two main subfamilies based on sequence identity and phylogenetic considerations: the $P2Y_1$ receptor subfamily, which is comprised of $P2Y_1$, $P2Y_2$, $P2Y_4$, $P2Y_6$, and $P2Y_{11}$ receptors, and the $P2Y_{12}$ receptor subfamily, comprising $P2Y_{12}$, $P2Y_{13}$, and $P2Y_{14}$ receptors. The $P2Y_1$ receptor subfamily is coupled to activation of phospholipase C, generation of inositol phosphates, activation of protein kinase C, and mobilization of intracellular Ca^{2+} stores. In addition to coupling to activation of phospholipase C, the $P2Y_{11}$ receptor is also coupled to G_s, thereby activating adenylyl cyclase (3–5). In contrast, the three members of the $P2Y_{12}$ receptor subfamily couple to $G_{i/o}$ and therefore inhibit adenylyl cyclase (6–8).

Although P2Y receptors mediate a multitude of cellular responses throughout the body, one of their main functions is to regulate ion transport in polarized epithelial cells. Proteins in polarized epithelial cells can be expressed predominantly at either the apical or basolateral membrane surface, or they can be indiscriminatingly distributed to both membranes. The proper targeting of proteins to their respective membrane surface is critical in host defense, nutrient absorption, ion transport, and signal transduction. However, the mechanism(s) by which epithelial cells target proteins to a particular membrane surface remains a critical question in epithelial cell biology.

Alterations in the trafficking and targeting of proteins are often associated with diseases (9–11). For example, cystic fibrosis, an autosomal recessive disease of the epithelia, is caused primarily by mutations that prevent expression of the cystic fibrosis transmembrane conductance regulator at the plasma membrane (12–14). This defect in cystic fibrosis transmembrane conductance regulator trafficking results in decreased Cl^- transport and water secretion, increased Na^+ absorption, and thickening of the mucous layer. The impairments caused by defective trafficking of the cystic fibrosis transmembrane conductance regulator can be alleviated acutely by activation of the $P2Y_2$ receptor (15–17). The $P2Y_2$ receptor is expressed in airway epithelial cells, and activation of this receptor from the apical surface increases Cl^- secretion and H_2O efflux through a cystic fibrosis transmembrane conductance regulator-independent mechanism (17), while at the same time decreasing Na^+ absorption by inhibiting epithelial sodium channels (18). Moreover, $P2Y_2$ receptor activation increases mucous secretion and ciliary beat frequency (19). Thus, activation of the $P2Y_2$ receptor facilitates mucociliary clearance and is an important therapeutic target for treatment of cystic fibrosis and other diseases of epithelia (20).

We have recently demonstrated by confocal microscopy that the $P2Y_2$ receptor is targeted to the apical membrane in epithelial cells of multiple lineages (21), and this localization is consistent with pharmacological studies of the receptor in epithelial cell lines (22, 23). Proteins are targeted to a particular membrane surface because they contain a signal within their primary sequence that is recognized by the cell. To reveal the location of the apical sorting signal of the $P2Y_2$ receptor, we utilized a chimeric receptor approach with the $P2Y_4$ receptor, which shares high sequence identity with the $P2Y_2$ receptor but achieves apical targeting by harboring an apical signal in its C-terminal tail. We show here that the apical targeting signal in the $P2Y_2$ receptor resides in its first extracellular loop and that four amino acids within this loop play a major role in directing apical targeting. This is the first report of an extracellular protein domain involved in apical targeting.

EXPERIMENTAL PROCEDURES

Construction of Chimeric and Mutant $P2Y_2$ and $P2Y_4$ Receptor cDNAs—Chimeric and mutant receptor cDNA constructs were gener-

* This work was supported by National Institutes of Health Grant R01 HL71131 (to R. A. N.). The costs of publication of this article were defrayed in part by the payment of page charges. This article must therefore be hereby marked "*advertisement*" in accordance with 18 U.S.C. Section 1734 solely to indicate this fact.

‡ To whom correspondence should be addressed: Dept. of Pharmacology, The University of North Carolina at Chapel Hill, CB 7365, Chapel Hill, NC 27599-7365. Tel.: 919-966-6547; Fax: 919-966-5640; E-mail: nicholas@med.unc.edu.

ated by overlap extension PCR (24) using *Pfu* polymerase (Stratagene, La Jolla, CA) and primers that incorporated an EcoRI restriction site at the 5′-end and a XhoI site at the 3′-end of the coding sequence. Truncated P2Y receptor constructs were generated by PCR with the same 5′ primers described above and 3′ primers that engineered a stop codon directly after the truncation site, followed by a XhoI site for cloning into pLXSN. $P2Y_2$ and $P2Y_4$ receptors were truncated at Arg^{315} and Tyr^{313}, respectively. For the BK2 receptor fusions, Phe^{316} of the $P2Y_2$ receptor and Asp^{311} of the $P2Y_4$ receptor were fused after Arg^{313} of the BK2 receptor. All receptor constructs were digested with EcoRI and XhoI and ligated into similarly digested pLXSN retroviral expression vectors. In addition, each of the cloned receptors harbored an HA[1]-epitope tag (YPYDVPDY) following the initiating methionine residue. Previous studies have shown that the presence of an HA epitope at the N terminus of the $P2Y_2$ receptor has no effect on its function (25).

Expression of Receptor Constructs in MDCK(II), 1321N1, and Caco-2 Cells—MDCK(II) (ATCC, Rockville, Maryland) cells were cultured in Dulbecco's modified Eagle's medium/F-12 (1:1) medium, Caco-2 cells in Earle's minimal essential medium with non-essential amino acids, and 1321N1 human astrocytoma cells in Dulbecco's modified Eagle's medium/high glucose medium. The culture medium was supplemented with either 5% fetal bovine serum (Hyclone, Gaithersburg, MD) for MDCK and 1321N1 cells or 20% fetal bovine serum for Caco-2 cells. Recombinant retrovirus particles were produced by calcium phosphate-mediated transfection of PA317 cells with the pLXSN vector containing the various receptor constructs, and the resultant viral particles were used to infect both MDCK(II) and 1321N1 cells (26). Geneticin-resistant cells were selected after 7–10 days with 0.6 mg ml^{-1} G418 and maintained in medium containing 0.4 mg ml^{-1} active G-418.

Confocal Microscopy—MDCK(II) and Caco-2 cells stably expressing HA-tagged receptor constructs were seeded in 12-mm polyester Transwell inserts (Corning Life Sciences, Acton, MA) and allowed to polarize for 7 days with daily medium changes. Cell monolayers were then washed with cold PBS^{2+} (containing 2 mM Ca^{2+} and Mg^{2+}), fixed with 2% paraformaldehyde for 30 min at 4 °C, and then permeabilized with −20 °C methanol for 1 min. Receptors were labeled with the anti-HA mouse monoclonal antibody HA.11 (Covance, Berkeley, CA) and the tight-junction protein complex was labeled with anti-ZO-1 rabbit polyclonal antibody (Zymed Laboratories Inc., South San Francisco, CA). Cells were washed 3 times with cold PBS^{2+} and labeled with goat anti-mouse A-488 (HA epitope) and goat anti-rabbit A-594 (ZO-1) secondary fluorescent antibodies (Molecular Probes, Eugene, OR). Following three more washes with cold PBS^{2+}, the Transwell filters containing the labeled and fixed monolayers were excised and mounted on glass microscope slides with Slowfade mounting medium (Molecular Probes).

Confocal microscopy was performed with an Olympus Fluoview 300 laser scanning confocal imaging system (Melville, NY) configured with an IX70 Fluorescence microscope fitted with a PlanApo ×60 oil objective. Two different views, an XY scan horizontal to the cell monolayer and an XZ scan vertical to the cell monolayer, were collected of all labeled monolayers to determine the steady-state localization of the receptor constructs. Representative results are shown for each construct.

Quantification of Cell Surface Expression of HA-tagged P2Y Receptors—MDCK(II) cells stably expressing HA-tagged P2Y receptors were seeded in duplicate in 24-mm Transwell inserts and allowed to polarize as described above. Monolayers were placed on ice and kept at 4 °C for the duration of the experiment. Cells were washed with cold PBS^{2+} three times for 5 min each, and then labeled with 1 mg/ml Sulfo-NHS-SS-Biotin (Pierce) in cold PBS^{2+} buffer, pH 8, for 40 min. The biotin solution was removed and the reaction quenched with 100 mM glycine in PBS^{2+} for 10 min. The cells were washed with PBS^{2+} and then incubated for 5 min with 0.7 ml of Tris-Triton buffer (50 mM Tris·HCl, pH 7.4, 100 mM NaCl, 5 mM EDTA, 1% Triton X-100) containing a protease inhibitor mixture. The cells were passed 7–10 times through a 25-gauge needle and then incubated for 1.5 h with rocking. The cell lysate was centrifuged at 20,000 × *g* for 30 min and the supernatant incubated with 50 ml of immobilized Neutravidin (Pierce) for 1.5 h. The resin was washed twice with Tris-Triton buffer and biotin-labeled proteins were eluted from the Neutravidin resin by incubating with 35 ml of SDS-PAGE sample buffer containing 100 mM dithiothreitol for 10 min at 37 °C. The dithiothreitol cleaves the disulfide bond within the biotin spacer and releases the proteins from Neutravidin under mild conditions.

Eluted proteins were separated by SDS-PAGE on a 10% gel and transferred overnight to polyvinylidene fluoride membranes. Membranes were blocked with 5% nonfat dry milk in PBS^{2+} for 1 h, then incubated with anti-HA monoclonal antibody conjugated to horseradish peroxidase (3F10; Roche Biochemicals, Indianapolis, IN). The blots were developed with SuperSignal West Pico chemiluminescent substrate (Pierce) and the resulting bands were imaged on a Bio-Rad Flour-S system and quantitated with Bio-Rad QuantityOne software (Bio-Rad). The % distribution values (based on the total protein expressed at the cell surface equaling 100%) reported in the text and figures represent the average of three independent experiments. The standard errors were <5% of the mean.

Radioimmunoassay for Detection of HA-tagged Receptors—1321N1 cells stably expressing HA-tagged $P2Y_2/P2Y_4$ chimeras were seeded at 10^5 cells/well in a 24-well plate. The expression of receptor chimeras was quantitated on confluent cells (~3 days after passage) essentially as described previously (48). Briefly, cells were fixed in 4% paraformaldehyde for 15 min at room temperature, after which they were washed twice with Hanks' balanced salt solution containing 1 mM each of Ca^{2+} and Mg^{2+} ($HBSS^{2+}$) and blocked with bovine serum albumin. Cells were incubated for 1 h at 37 °C with a 1:1000 dilution of mouse anti-HA monoclonal antibody (clone HA.11; Covance Research Products, Denver, PA). Cells were washed twice with $HBSS^{2+}$, followed by addition of ^{125}I-labeled rabbit anti-mouse antibody (typically 10^5 cpm/well). After a 2-h incubation at room temperature, the cells were washed twice with $HBSS^{2+}$. Cells were then solubilized overnight with 1 M NaOH and transferred to glass tubes for quantitation of radioactivity by γ-counting.

Intracellular [Ca^{2+}] Measurements—Agonist-promoted increases in intracellular [Ca^{2+}] were quantified under constant superfusion in 1321N1 cells stably expressing HA-tagged $P2Y_2/P2Y_4$ chimeras as described previously (27). UTP (100 μM) was applied for 30 s in the superfusate (1.4 ml/min) and increases in intracellular [Ca^{2+}] were measured in 6–13 individual cells per coverslip. To avoid receptor desensitization, each coverslip was challenged with UTP only once. The average responses from 6 to 13 cells per coverslip were measured from three coverslips. Data were recorded and processed using an InCyt IM2 digital imaging system (Intracellular Imaging Inc., Cincinnati, OH).

Assay of Inositol Phosphate Accumulation—1321N1 human astrocytoma cells stably expressing the $P2Y_2$ receptor constructs were seeded in 24-well plates at 1×10^5 cells/well and assayed 3 days later when confluent. Inositol lipids were radiolabeled by incubating the cells with 200 μl of serum-free, inositol-free DMEM containing 0.4 mCi of *myo*-[^3H]inositol. UTP was added at 5× concentration in 50 ml of 50 mM LiCl, 250 mM HEPES, pH 7.25. Following a 5-min incubation at 37 °C, the medium was aspirated and the reaction was terminated by adding 0.75 ml boiling EDTA, pH 8.0. [^3H]Inositol phosphates were resolved on Dowex AG1-X8 columns as described (5).

RESULTS

Role of the C-terminal Tail in the Apical Targeting of $P2Y_2$ and $P2Y_4$ Receptors—We have shown previously that the $P2Y_2$ receptor, when expressed in MDCK(II) epithelial cells, is located exclusively at the apical membrane at steady state (21) (Fig. 1*A*). To determine the location of the signal that directs apical targeting, we first examined the targeting of the $P2Y_2$ receptor missing its C-terminal tail and the B2-bradykinin receptor in which its C-terminal tail was replaced by the C-tail of the $P2Y_2$ receptor. We focused on the C-terminal tail because several 7TM receptors, including rhodopsin (28), three peptide hormone receptors (thyroid stimulating hormone, leutinizing hormone, and follicle-stimulating hormone receptors) (29–31), and the $P2Y_1$ receptor,[2] achieve polarized expression because of sequences within their C-terminal tails. As shown in Fig. 1*A*, both the full-length $P2Y_2$ receptor and the receptor missing its C-tail ($P2Y_2$-ΔCT) were expressed exclusively at the apical membrane of MDCK(II) cells. Moreover, replacement of the

[1] The abbreviations used are: HA, hemagglutinin; 7TM, seven transmembrane; BK2, bradykinin 2 receptor; EL1 and EL2, 1st and 2nd extracellular loop respectively; $P2Y_2$-ΔCT, the $P2Y_2$ receptor missing its C-terminal tail; $P2Y_4$-ΔCT, the $P2Y_4$ receptor missing its C-terminal tail; PDZ, postsynaptic density protein of 95-kDa disc large-zona occludens; PBS, phosphate-buffered saline; MDCK, Madin-Darby canine kidney.

[2] S. C. Wolff, A.-D. Qi, and R. A. Nicholas, manuscript in preparation.

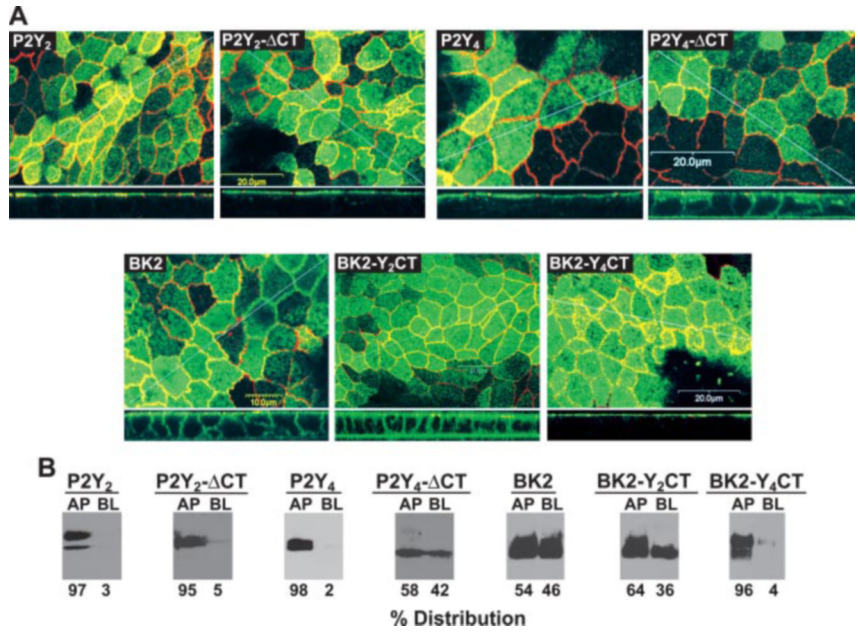

FIG. 1. **The C-terminal tail of the P2Y$_2$ receptor is not involved in apical targeting.** *A*, confocal micrographs of polarized MDCK(II) cells expressing HA-tagged receptor constructs. The localization of the HA-tagged receptors (*green fluorescence*) was determined by examining receptor expression relative to the tight-junction protein complex (*red fluorescence*), which demarcates the apical and basolateral membrane surfaces. Confocal images were generated by scanning both parallel (XY, *top*) and perpendicular (XZ, *bottom*) to the monolayer. The *white line* in the XY scan indicates the position where the XZ scan was taken. *B*, relative distribution of receptor constructs at the apical (*AP*) or basolateral (*BL*) surface was determined by a polarized biotinylation procedure as described under "Experimental Procedures." The total protein expressed on the cell surface was taken to be 100%. Representative blots are shown but the *numbers* underneath each lane reflect the average relative distribution determined from a minimum of three independent experiments.

C-terminal tail of the B2-bradykinin (BK2) receptor, which is unsorted in MDCK(II) cells, with the C-terminal tail of the P2Y$_2$ receptor had no effect on targeting (Fig. 1*B*). These data, which were confirmed in biotinylation experiments (Fig. 1*C*), demonstrated that the P2Y$_2$ receptor contains an apical targeting signal within the region comprising the N terminus through TM7.

The P2Y$_4$ receptor, which has the highest sequence identity to the P2Y$_2$ receptor of all the members in the P2Y receptor family, is also expressed at the apical membrane of MDCK(II) cells (21) (Fig. 1*A*). In contrast to the P2Y$_2$ receptor, however, the P2Y$_4$ receptor missing its C-terminal tail (P2Y$_4$-ΔCT) was unsorted, whereas the BK2 receptor containing the C-terminal tail of the P2Y$_4$ receptor was expressed at the apical membrane (Fig. 1, *A* and *B*). Importantly, the BK2 receptor missing its C-terminal tail was unsorted (data not shown), confirming that the apical location of the BK2-P2Y$_4$ CT receptor was due to the addition of the P2Y$_4$ C-terminal tail and not to the uncovering of a cryptic apical signal in the BK2 receptor missing its C-terminal tail. The localization of these receptors identified by confocal microscopy was also verified by biotinylation (Fig. 1*C*). These data demonstrated that the P2Y$_4$ receptor, although highly homologous to the P2Y$_2$ receptor, achieves apical targeting by a different mechanism, by having an apical targeting signal in its C-terminal tail. A more in depth characterization of the P2Y$_4$ receptor apical targeting signal will be reported in a separate study.

Characterization of P2Y$_2$/P2Y$_4$-ΔCT Receptor Chimeras—The results described above suggested that P2Y$_2$/P2Y$_4$ receptor chimeras, in which the apical signal within the C-tail of the P2Y$_4$ receptor was removed, would allow us to define the location of the apical targeting signal within the P2Y$_2$ receptor. P2Y$_2$ and P2Y$_4$ receptors have 52% sequence identity overall, which increases to 63% when comparing sequences between TM1 through TM7. Thus, we generated a series of chimeras starting with the P2Y$_2$ receptor and progressively containing increasing amounts of P2Y$_4$-ΔCT sequence at the C terminus (Fig. 2*A*). We hypothesized that the general location of the apical targeting signal in the P2Y$_2$ receptor would be revealed when the region of the P2Y$_2$ receptor containing the signal was replaced with the corresponding P2Y$_4$ receptor sequence.

To exclude the possibility that these chimeric receptors might be non-functional and therefore show aberrant targeting, we expressed the P2Y$_2$/P2Y$_4$-ΔCT receptor chimeras in 1321N1 human astrocytoma cells and measured intracellular Ca^{2+} mobilization in response to 100 μM UTP, a common agonist of the two receptors. 1321N1 cells were utilized for this purpose as they do not endogenously express G_q-coupled P2Y receptors, whereas MDCK(II) cells express canine homologues of P2Y$_1$, P2Y$_2$, and P2Y$_{11}$ receptors that would complicate functional analysis (32). As shown in Fig. 2*A*, each of the five receptor chimeras mobilized intracellular Ca^{2+}, although the responses promoted by the last two chimeras (4 and 5) were considerably lower than those promoted by chimeras 1–3. The lower responses of chimeras 4 and 5 were due at least in part to a decrease in cell surface expression, as a cell surface radioimmunoassay revealed that these constructs were expressed at 20–40% of the levels of the other chimeras (Fig. 2*A*, *inset*). Taken together, these data demonstrate that each of the receptor chimera constructs was functional.

The first three P2Y$_2$/P2Y$_4$-ΔCT receptor chimeras, which contain the least amount of P2Y$_4$ receptor sequence, were localized to the apical membrane of MDCK(II) cells (Fig. 2*B*). In addition, intense staining for two of these constructs (chimeras 1 and 2) was observed just below the apical membrane. In contrast to chimeras 1–3, apical targeting was lost when the additional P2Y$_2$ receptor sequence from the 1st extracellular loop (EL1) through TM3 was replaced with the corresponding sequence from the P2Y$_4$ receptor (chimera 4), suggesting that the apical targeting signal of the P2Y$_2$ receptor is located within this region (Fig. 2*B*). A similar loss of targeting was observed in chimera 5, which also contains the EL1—TM3 sequence from the P2Y$_4$ receptor. Chimeras 4 and 5 also showed a considerable amount of diffuse staining underneath the membrane surface.

Identification of the Amino Acids in the P2Y$_2$ Receptor Involved in Apical Targeting—There are nine amino acid differences in EL1 and TM3 between the P2Y$_2$ and P2Y$_4$ receptor, seven of which are located within EL1 (Fig. 3*A*). To determine which of these amino acids are critical for apical targeting, we mutated the full-length P2Y$_2$ receptor, three amino acids at a time, to the corresponding residues of the P2Y$_4$ receptor. The mutant receptors (Arg^{95}-Gly^{96}-Asp^{97} → AHN, Ser^{102}-Val^{104}-Leu^{105} → GEI, and Leu^{108}-Thr^{115}-Ile^{121} → FWV) were expressed in MDCK(II) cells and their steady-state localization was determined (Fig. 3*B*). Both the RGD and LTI triple mutant

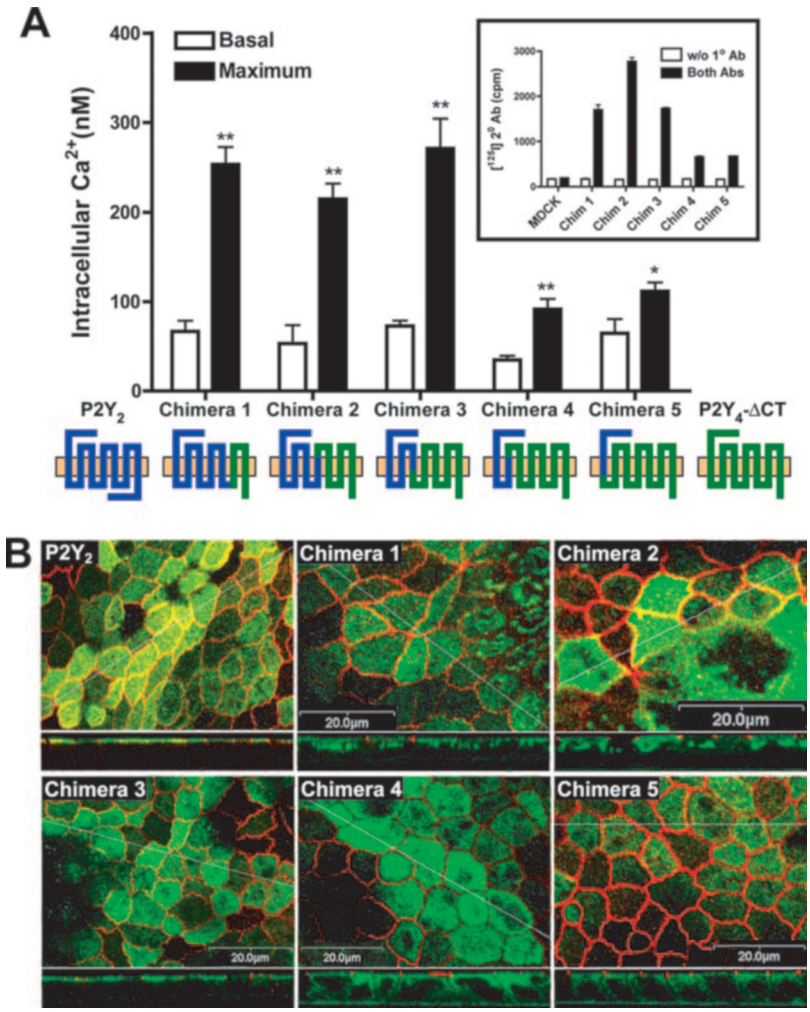

FIG. 2. **P2Y$_2$/P2Y$_4$ receptor chimeras allow localization of the apical targeting signal of the P2Y$_2$ receptor.** *A*, the functional activity of chimeras 1–5 was assessed following expression in 1321N1 cells. Cells were plated on coverslips and the increase in intracellular [Ca^{2+}] in response to 100 μM UTP was monitored in 6–13 cells on a coverslip under constant superfusion (27). The peak [Ca^{2+}] averaged from 3 separate coverslips is shown before (*basal*) and after (*maximum*) challenge with UTP. *, $p < 0.05$; **, $p < 0.01$ compared to basal level by paired *t*-test. *Inset*, cell surface radioimmunoassay of HA-tagged chimeras 1–5 expressed in MDCK cells. The receptor schematics show the approximate junctions of the two receptors in each chimera. *B*, confocal micrographs of the P2Y$_2$ receptor and chimeras 1–5 expressed in MDCK(II) cells.

receptors were unsorted, with nearly 40% of the receptors expressed on the basolateral surface (Fig. 3*D*). In contrast, the SVL triple mutant receptor was still mostly expressed at the apical membrane, with only very light staining in the lateral membranes below the tight junctions, suggesting that these three amino acids play a very minor role in targeting (Fig. 3*B*).

Further elaboration of the two triple mutant receptors was accomplished by making six individual mutations in the full-length P2Y$_2$ receptor, again to the corresponding residue in the P2Y$_4$ receptor. As shown in Fig. 3*C*, mutation of Arg^{95}, Gly^{96}, Asp^{97}, or Leu^{108} resulted in an unsorted phenotype, with 30–36% of the receptors localized to the basolateral surface, whereas mutation of Ile^{121} (14% basolateral) and Thr^{115} (6% basolateral) had little to no effect on targeting. Taken together, these data identify four amino acids that play a critical role in apical targeting of the P2Y$_2$ receptor.

The Role of Integrins in Apical Targeting of the P2Y$_2$ Receptor—The RGD triad is a well known integrin-binding motif (33), and the $\alpha_V\beta_3$ integrin has been reported to interact with the RGD motif of the human P2Y$_2$ receptor and to modify its signaling properties (34). As shown in Fig. 3*C*, mutation of any one of the three residues in the RGD motif of the P2Y$_2$ receptor generated an unsorted phenotype. Thus, it was possible that interaction with integrins through the RGD motif of the P2Y$_2$ receptor is responsible for apical targeting. To test this possibility, we constructed two mutations in the full-length human P2Y$_2$ receptor that disrupted the RGD integrin-binding motif: RGD → QGD which is the sequence of the rat P2Y$_2$ receptor in this region, and RGD → RGE. When expressed in MDCK(II) cells, both the QGD and RGE mutant P2Y$_2$ receptors targeted exclusively to the apical membrane (Fig. 4). These data provide compelling evidence that intergrins are not involved in apical targeting of the P2Y$_2$ receptor.

Targeting of P2Y$_2$ Receptor Mutants in Human Caco-2 Epithelial Cells—We showed previously that the G_q-coupled P2Y receptors, including the P2Y$_2$ receptor, are targeted in a similar fashion in MDCK and Caco-2 epithelial cells (21). To confirm that the amino acids involved in targeting of the P2Y$_2$ receptor function in an identical manner in other epithelial cells, we expressed in Caco-2 cells the wild-type P2Y$_2$ receptor and the four mutants (R95A, G96H, D97N, and L108F) that disrupt targeting in MDCK cells (Fig. 3*C*), and examined their steady-state distribution by confocal microscopy. As in MDCK cells, the wild-type P2Y$_2$ receptor in Caco-2 cells was targeted to the apical membrane, whereas the four mutant receptors were non-sorted (Fig. 5). Thus, these amino acids likely utilize identical mechanisms to promote apical targeting in two different epithelial cell lines.

Functional Activities of P2Y$_2$ Receptor Mutants—A potential caveat to our mutational analysis was that the mutations might result in non-functional receptors and cause aberrant targeting. To test the functional activity of our P2Y$_2$ receptor mutants, we expressed each receptor in 1321N1 human astrocytoma cells and generated concentration-effect curves for UTP-promoted [^{3}H]inositol phosphate accumulation. As shown in Fig. 6, each of the receptor mutants, with the exception of the RGD → RGE mutant, showed similar EC_{50} values for UTP and maximal [^{3}H]inositol phosphate levels. The RGD → RGE mu-

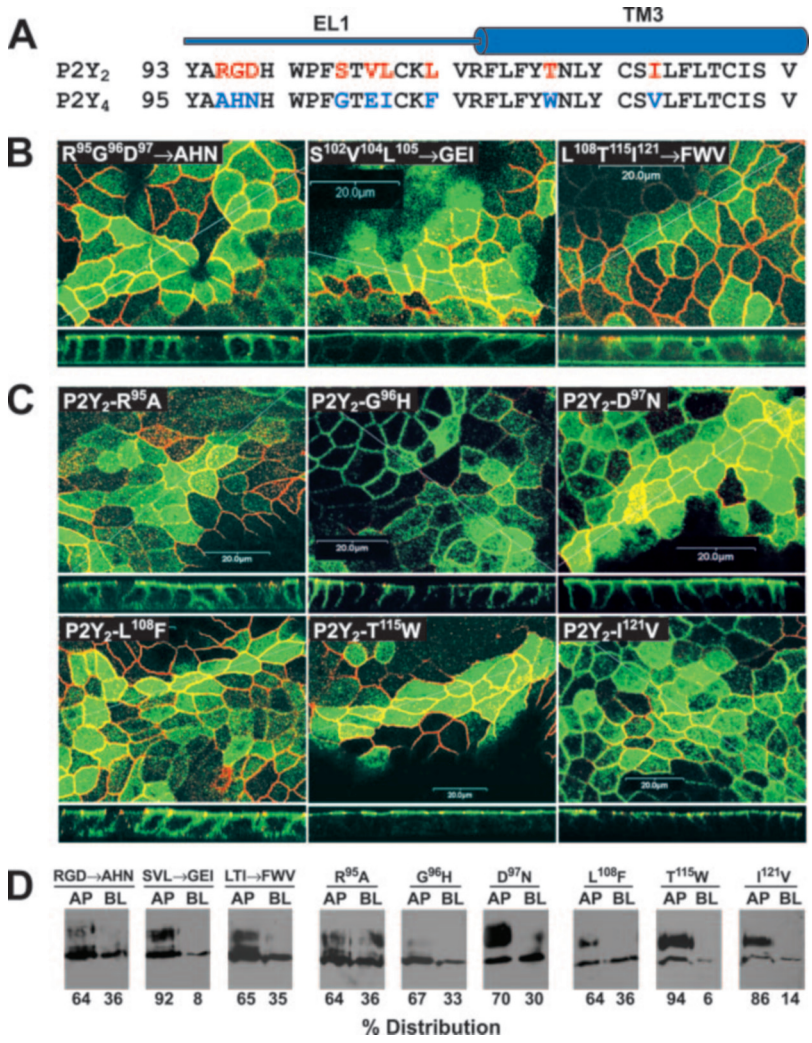

FIG. 3. **Four residues within EL1 are important in apical targeting of the P2Y$_2$ receptor.** *A*, alignment of the EL1/TM3 regions of P2Y$_2$ and P2Y$_4$ receptors. Different amino acids between the two receptors are shown in *red* (P2Y$_2$) or *blue* (P2Y$_4$). *B*, confocal micrographs of MDCK(II) cells expressing HA-P2Y$_2$ receptors harboring the indicated triple mutations in EL1/TM3. *C*, confocal micrographs of MDCK(II) cells expressing HA-P2Y$_2$ receptors with the indicated single mutations. *D*, relative distribution of receptor constructs at the apical (*AP*) or basolateral (*BL*) surface as determined by a polarized biotinylation procedure.

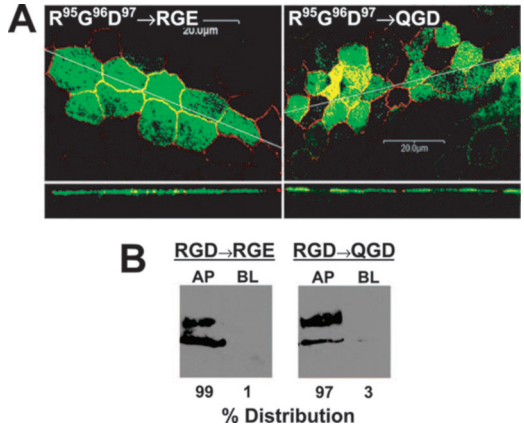

FIG. 4. **Integrins are not involved in directing apical targeting of the P2Y$_2$ receptor.** To determine the possible involvement of integrins in apical targeting of the P2Y$_2$ receptor, the RGD sequence of the P2Y$_2$ receptor was mutated to either RGE or QGD. *A*, confocal micrographs of polarized MDCK(II) cells expressing the indicated HA-P2Y$_2$ receptor mutants. *B*, relative distribution of receptor constructs at the apical (*AP*) or basolateral (*BL*) surface as determined by a polarized biotinylation procedure.

tant receptor was also active, but the EC$_{50}$ of UTP was shifted nearly 3 orders of magnitude to the right. These data discount the possibility that the loss of apical targeting in the EL1 mutants of the P2Y$_2$ receptor is because of production of nonfunctional receptors, and highlight the role of amino acids in EL1 in apical targeting of the P2Y$_2$ receptor.

DISCUSSION

Sorting signals for apically targeted membrane proteins are relatively diverse. These signals include glycophosphatidylinositol anchoring, *N*- and *O*-linked glycosylation, PDZ-binding motifs, intracellular motifs, and even transmembrane domains (9, 35, 36). To determine the identity and location of the sorting signal for the P2Y$_2$ receptor, we utilized chimeras between P2Y$_2$ and P2Y$_4$ receptors, which have high homology but contain apical sorting signals in distinct regions, and P2Y$_2$ receptors with point mutations. These mutant receptor constructs, with few exceptions, were expressed at the cell surface at wild type levels and were fully active, eliminating concern that mistargeting was due to the receptor being non-functional or misfolded. We showed that the P2Y$_2$ receptor achieves apical targeting at least in part by sequences in EL1. In particular, four amino acids (Arg^{95}, Gly^{96}, Asp^{97}, and Leu^{108}) within EL1 appear to be critical in apical targeting, as mutation of these residues to their counterparts in the P2Y$_4$ receptor resulted in an unsorted distribution in MDCK(II) cells. Thus, the present study increases the diversity of apical signals by showing that an extracellular protein sequence also can function as a targeting signal.

This is also one of a few studies to focus on the targeting signals directing polarized sorting of 7TM receptors. In fact, targeting signals have being identified and characterized in only six 7-TM receptors. These include rhodopsin and 5-HT$_{1B}$ receptors, which contain an apical targeting signal in their C-terminal tails, three hormone receptors (the thyrotropin,

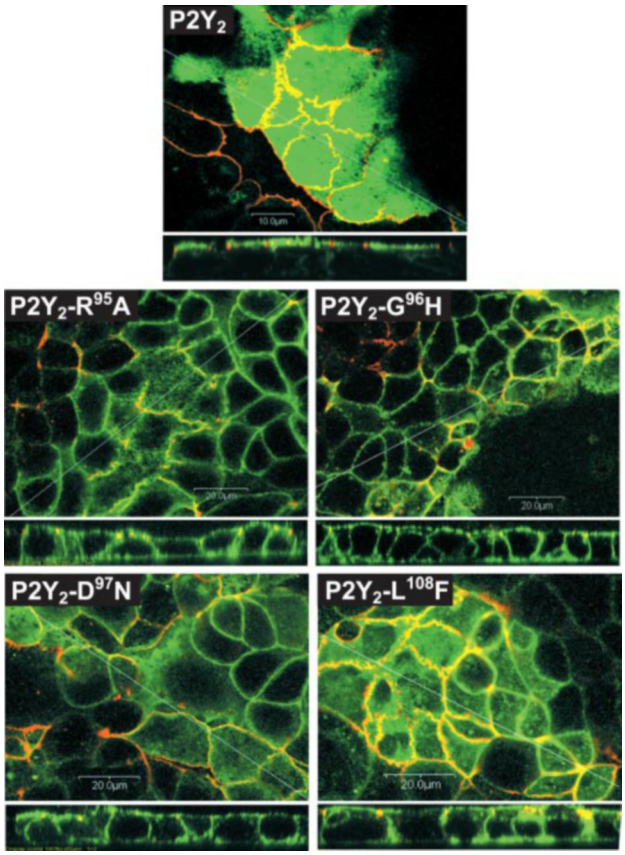

FIG. 5. **The apical targeting signal of the P2Y$_2$ receptor functions in Caco-2 cells.** To determine whether targeting of P2Y receptors was dependent on the cell line in which they were expressed, wild-type and four mutant P2Y receptors (R95A, G96H, D97N, and L108F) were expressed in Caco-2 cells and the steady-state distribution of the receptors was analyzed by confocal microscopy.

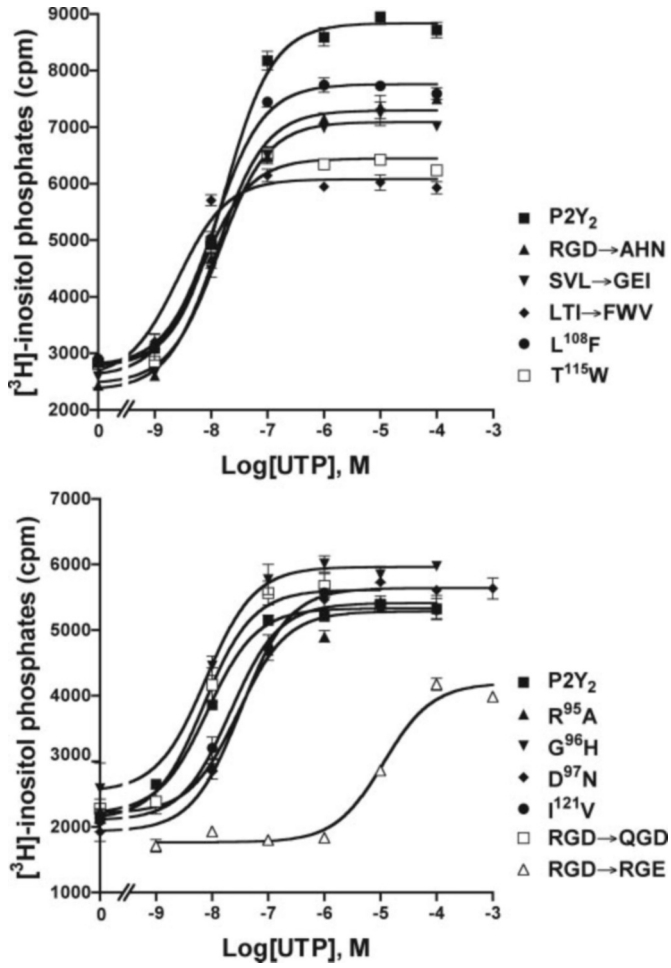

FIG. 6. **The P2Y$_2$ receptor mutants are functional.** Wild type and mutant P2Y$_2$ receptors were expressed individually in 1321N1 cells, a cell line that does not show an endogenous response to nucleotides, and their functional activities were assessed by quantitating nucleotide-promoted inositol phosphates accumulation. Data shown are the mean ± S.D. of triplicate assays from three separate experiments.

lutenizing hormone, and follicle stimulating hormone receptors), which contain a basolateral targeting signal in their C-terminal tails, and the M_3-muscarinic receptor, which contains a basolateral targeting signal in its 3rd intracellular loop (28, 31, 37, 38). A recent study with P2Y receptors demonstrated that 7 of the 8 P2Y receptors (P2Y$_1$, P2Y$_2$, P2Y$_4$, P2Y$_6$, P2Y$_{11}$, P2Y$_{12}$, and P2Y$_{14}$) show a polarized distribution in kidney, lung, and colon epithelial cells (21). These data suggest that the seven polarized receptors harbor targeting signals that direct localization to one of the two distinct membrane surfaces in epithelial cells. Thus, in addition to the P2Y$_2$ receptor, other P2Y receptors may provide considerable new insight regarding the location and identity of targeting signals in 7TM receptors.

Demonstration of a sorting signal in the C-terminal tail of a 7TM receptor is relatively straightforward. For example, by examining the membrane localization of the P2Y$_4$ receptor missing its C-terminal tail and the normally unsorted BK2 receptor in which its C-terminal tail was replaced with the C-terminal tail of the P2Y$_4$ receptor, we illustrated with high confidence that the C-terminal tail of the P2Y$_4$ receptor directs apical targeting (Fig. 1). In contrast, the P2Y$_2$ receptor achieves apical targeting via a targeting signal located between the N terminus and the end of the 7TM (Fig. 1). This region is critically involved in receptor function, stability, cell surface expression and/or proper folding, and therefore, identification of an "internal" targeting sequence is difficult by standard techniques. Indeed, an exhaustive search for the basolateral targeting sequence of the α_{2A} adrenergic receptor failed to identify a particular sequence or region involved in targeting (39). To circumvent these constraints, we took advantage of the high homology between the P2Y$_2$ and P2Y$_4$ receptors (52% identity) and the distinct mechanisms by which they reach the apical surface to identify a unique apical targeting signal in EL1 of the P2Y$_2$ receptor.

We have identified residues in EL1 of the P2Y$_2$ receptor that are involved in apical targeting. However, it is not clear whether the entire signal is contained within EL1 or whether other regions of the receptor are also involved. We addressed this question by constructing a chimera of the P2Y$_4$-ΔCT receptor that contained EL1 of the P2Y$_2$ receptor, in an attempt to make a "gain-of-function" mutant. Unfortunately, this chimera was not expressed at the cell surface (data not shown) and further investigation was not pursued. Interestingly, the apical signal is located near Cys^{106}, which forms a disulfide bond with Cys^{183} in EL2 that is critical for cell surface expression in the P2Y$_1$ (40), β-adrenergic (41), and many other receptors.

The Arg^{95}-Gly^{96}-Asp^{97} sequence, which we have shown is clearly involved in apical targeting of the P2Y$_2$ receptor, is also a well known integrin-binding motif (33). In epithelial cells, most integrins are β1 heterodimers, including α1β1, α2β1, α6β1, and α3β1, although some epithelial cells may also express α6β4, an epithelial-specific integrin, and α5β1 and αvβ3 (42, 43). The RGD sequence of the P2Y$_2$ receptor has been reported to interact with integrins and to regulate the signaling properties of the receptor (34). Thus, it was conceivable that

the P2Y$_2$ receptor becomes localized to the apical surface by virtue of the interaction of its RGD sequence with an apically localized integrin. However, mutation of the RGD motif of the P2Y$_2$ receptor to RGE, which abolishes integrin interaction (44), or to QGD, which is the only divergent amino acid residue in EL1 between the human and rat homologues, had no effect on apical targeting (Fig. 4). These data provide strong evidence that integrins are not involved in apical targeting of the P2Y$_2$ receptor.

All of the receptors examined showed similar EC_{50} values for UTP-promoted [^{3}H]inositol phosphate accumulation with the exception of the RGD → RGE mutant. UTP was less potent by 3 orders of magnitude at this mutant receptor than at the wild type P2Y$_2$ receptor. A similar shift to the right in EC_{50} was observed by Erb *et al.* (34), who attributed the decrease in potency to disruption of binding of the P2Y$_2$ receptor to the $\alpha v\beta 3$ integrin. However, we have shown that extracellular mutations dramatically influence the EC_{50} and specificity of nucleotides in the P2Y$_4$ receptor (45), and another study on the P2Y$_1$ receptor highlighted the role of extracellular determinants in ligand binding and activation (46). Moreover, UTP activated both the RGD → AHN and RGD → QGD mutants with essentially identical EC_{50} values as the wild type P2Y$_2$ receptor (Fig. 6). Because these mutants no longer contain the RGD motif and therefore are not capable of binding integrins, it seems more likely that the decrease in potency in the D97E mutant is due to changes in its capacity to be activated by UTP and not to effects caused by the lack of presumptive binding to integrins.

The observation that the protein trafficking machinery recognizes an extracellular targeting signal in the P2Y$_2$ receptor is difficult to reconcile with the concept that once the receptor is synthesized, the signal becomes inaccessible to cytoplasmic components. Schuck and Simons (35) have proposed that apical expression is driven at least in part by the propensity of a protein to reside within lipid rafts that are abundant in the apical membrane. In addition, oligomerization was suggested to increase the affinity of proteins for lipid rafts, thus also implicating oligomerization domains in apical targeting. However, in the three-dimensional structure of rhodopsin (47), EL1 folds into the center of the receptor and forms a disulfide linkage with EL2. Very little of EL1 is exposed at the outer surface of the receptor, which would make it unavailable for interaction with lipids or other receptors. Thus, although it is conceivable that lipid raft association or oligomerization underlies apical targeting, our results are more consistent with a co-translational sorting mechanism as a means by which the P2Y$_2$ receptor reaches the apical membrane. Current studies are focused on whether the P2Y$_2$ receptor is sorted intracellularly and delivered directly to the apical surface or whether delivery of the receptor to both membrane surfaces, coupled with an increased stability at the apical membrane, underlies its steady-state apical expression.

Acknowledgments—We thank Ken Harden for enthusiastic support, advice, and critical reading of the manuscript. We also acknowledge JoAnn Trejo and members of the Trejo and Harden labs for many comments and suggestions. Many thanks to Izabela Naruszewicz and Desiree Germain for excellent technical support.

REFERENCES

1. Harden, T. K. (1998) in *Cardiovascular Biology of Purines* (Burnstock, G., Dobson, J. G. J., Liang, B. T., and Linden, J., eds) pp. 187–206 Kluwer Academic Publishers, London
2. Ralevic, V., and Burnstock, G. (1998) *Pharmacol. Rev.* **50,** 413–492
3. Torres, B., Zambon, A. C., and Insel, P. A. (2002) *J. Biol. Chem.* **277,** 7761–7765
4. Communi, D., Govaerts, C., Parmentier, M., and Boeynaems, J. M. (1997) *J. Biol. Chem.* **272,** 31969–31973
5. Qi, A. D., Kennedy, C., Harden, T. K., and Nicholas, R. A. (2001) *Br. J. Pharmacol.* **132,** 318–326
6. Hollopeter, G., Jantzen, H. M., Vincent, D., Li, G., England, L., Ramakrishnan, V., Yang, R. B., Nurden, P., Nurden, A., Julius, D., and Conley, P. B. (2001) *Nature* **409,** 202–207
7. Communi, D., Gonzalez, N. S., Detheux, M., Brezillon, S., Lannoy, V., Parmentier, M., and Boeynaems, J. M. (2001) *J. Biol. Chem.* **276,** 41479–41485
8. Chambers, J. K., Macdonald, L. E., Sarau, H. M., Ames, R. S., Freeman, K., Foley, J. J., Zhu, Y., McLaughlin, M. M., Murdock, P., McMillan, L., Trill, J., Swift, A., Aiyar, N., Taylor, P., Vawter, L., Naheed, S., Szekeres, P., Hervieu, G., Scott, C., Watson, J. M., Murphy, A. J., Duzic, E., Klein, C., Bergsma, D. J., Wilson, S., and Livi, G. P. (2000) *J. Biol. Chem.* **275,** 10767–10771
9. Altschuler, Y., Hodson, C., and Milgram, S. L. (2003) *Curr. Opin. Cell Biol.* **15,** 423–429
10. Koivisto, U. M., Hubbard, A. L., and Mellman, I. (2001) *Cell* **105,** 575–585
11. Toye, A. M., Banting, G., and Tanner, M. J. (2004) *J. Cell Sci.* **117,** 1399–1410
12. Kerem, B., Rommens, J. M., Buchanan, J. A., Markiewicz, D., Cox, T. K., Chakravarti, A., Buchwald, M., and Tsui, L. C. (1989) *Science* **245,** 1073–1080
13. Riordan, J. R., Rommens, J. M., Kerem, B., Alon, N., Rozmahel, R., Grzelczak, Z., Zielenski, J., Lok, S., Plavsic, N., and Chou, J. L. (1989) *Science* **245,** 1066–1073
14. Rommens, J. M., Iannuzzi, M. C., Kerem, B., Drumm, M. L., Melmer, G., Dean, M., Rozmahel, R., Cole, J. L., Kennedy, D., and Hidaka, N. (1989) *Science* **245,** 1059–1065
15. Donaldson, S. H., and Boucher, R. C. (1997) in *The P2 Nucleotide Receptors* (Turner, J. T., Weisman, G. A., and Fedan, J. S., eds) Humana Press, Inc., Totowa, NJ
16. Paradiso, A. M., Ribeiro, C. M., and Boucher, R. C. (2001) *J. Gen. Physiol.* **117,** 53–67
17. Knowles, M. R., Clarke, L. L., and Boucher, R. C. (1991) *N. Engl. J. Med.* **325,** 533–538
18. Mall, M., Wissner, A., Gonska, T., Calenborn, D., Kuehr, J., Brandis, M., and Kunzelmann, K. (2000) *Am. J. Respir. Cell Mol. Biol.* **23,** 755–761
19. Bennett, W. D., Olivier, K. N., Zeman, K. L., Hohneker, K. W., Boucher, R. C., and Knowles, M. R. (1996) *Am. J. Respir. Crit. Care Med.* **153,** 1796–1801
20. Yerxa, B. R., Sabater, J. R., Davis, C. W., Stutts, M. J., Lang-Furr, M., Picher, M., Jones, A. C., Cowlen, M., Dougherty, R., Boyer, J., Abraham, W. M., and Boucher, R. C. (2002) *J. Pharmacol. Exp. Ther.* **302,** 871–880
21. Wolff, S. C., Qi, A. D., Harden, T. K., and Nicholas, R. A. (2005) *Am. J. Physiol.* **288,** C624–C632
22. Cressman, V. L., Lazarowski, E., Homolya, L., Boucher, R. C., Koller, B. H., and Grubb, B. R. (1999) *J. Biol. Chem.* **274,** 26461–26468
23. McAlroy, H. L., Ahmed, S., Day, S. M., Baines, D. L., Wong, H. Y., Yip, C. Y., Ko, W. H., Wilson, S. M., and Collett, A. (2000) *Br. J. Pharmacol.* **131,** 1651–1658
24. Ho, S. N., Hunt, H. D., Horton, R. M., Pullen, J. K., and Pease, L. R. (1989) *Gene* (*Amst.*)**77,** 51–59
25. Sromek, S. M., and Harden, T. K. (1998) *Mol. Pharmacol.* **54,** 485–494
26. Comstock, K. E., Watson, N. F., and Olsen, J. C. (1997) in *Methods in Molecular Biology: Recombinant Gene Expression Protocols* (Tuan, R., ed) Vol. 62, pp. 207–222, Humana Press, Totowa, NJ
27. Kennedy, C., Qi, A. D., Herold, C. L., Harden, T. K., and Nicholas, R. A. (2000) *Mol. Pharmacol.* **57,** 926–931
28. Chuang, J. Z., and Sung, C. H. (1998) *J. Cell Biol.* **142,** 1245–1256
29. Beau, I., Misrahi, M., Gross, B., Vannier, B., Loosfelt, H., Hai, M. T., Pichon, C., and Milgrom, E. (1997) *J. Biol. Chem.* **272,** 5241–5248
30. Beau, I., Groyer-Picard, M. T., Le Bivic, A., Vannier, B., Loosfelt, H., Milgrom, E., and Misrahi, M. (1998) *J. Biol. Chem.* **273,** 18610–18616
31. Beau, I., Groyer-Picard, M. T., Desroches, A., Condamine, E., Leprince, J., Tome, J. P., Dessen, P., Vaudry, H., and Misrahi, M. (2004) *Mol. Endocrinol.* **18,** 733–746
32. Insel, P. A., Ostrom, R. S., Zambon, A. C., Hughes, R. J., Balboa, M. A., Shehnaz, D., Gregorian, C., Torres, B., Firestein, B. L., Xing, M., and Post, S. R. (2001) *Clin. Exp. Pharmacol. Physiol.* **28,** 351–354
33. Ruoslahti, E. (1996) *Annu. Rev. Cell Dev. Biol.* **12,** 697–715
34. Erb, L., Liu, J., Ockerhausen, J., Kong, Q., Garrad, R. C., Griffin, K., Neal, C., Krugh, B., Santiago-Perez, L. I., Gonzalez, F. A., Gresham, H. D., Turner, J. T., and Weisman, G. A. (2001) *J. Cell Biol.* **153,** 491–501
35. Schuck, S., and Simons, K. (2004) *J. Cell Sci.* **117,** 5955–5964
36. Dunbar, L. A., Aronson, P., and Caplan, M. J. (2000) *J. Cell Biol.* **148,** 769–778
37. Nadler, L. S., Kumar, G., and Nathanson, N. M. (2001) *J. Biol. Chem.* **276,** 10539–10547
38. Jolimay, N., Franck, L., Langlois, X., Hamon, M., and Darmon, M. (2000) *J. Neurosci.* **20,** 9111–9118
39. Saunders, C., Keefer, J. R., Bonner, C. A., and Limbird, L. E. (1998) *J. Biol. Chem.* **273,** 24196–24206
40. Moro, S., Hoffmann, C., and Jacobson, K. A. (1999) *Biochemistry* **38,** 3498–3507
41. Dohlman, H. G., Caron, M. G., DeBlasi, A., Frielle, T., and Lefkowitz, R. J. (1990) *Biochemistry* **29,** 2335–2342
42. Matlin, K. S., Haus, B., and Zuk, A. (2003) *Methods* **30,** 235–246
43. Schoenenberger, C. A., Zuk, A., Zinkl, G. M., Kendall, D., and Matlin, K. S. (1994) *J. Cell Sci.* **107,** 527–541
44. Cherny, R. C., Honan, M. A., and Thiagarajan, P. (1993) *J. Biol. Chem.* **268,** 9725–9729
45. Herold, C. L., Qi, A. D., Harden, T. K., and Nicholas, R. A. (2004) *J. Biol. Chem.* **279,** 11456–11464
46. Hoffmann, C., Moro, S., Nicholas, R. A., Harden, T. K., and Jacobson, K. A. (1999) *J. Biol. Chem.* **274,** 14639–14647
47. Palczewski, K., Kumasaka, T., Hori, T., Behnke, C. A., Motoshima, H., Fox, B. A., Le Trong, I., Teller, D. C., Okada, T., Stenkamp, R. E., Yamamoto, M., and Miyano, M. (2000) *Science* **289,** 739–745
48. Brinson, A. E., and Harden, T. K.. (2001) *J. Biol. Chem.* **276,** 11939–11948